Food Research International 226 (2026) 118215

Contents lists available at ScienceDirect

Food Research International

journal homepage: www.elsevier.com/locate/foodres

Air-liquid interface biofilm formation of pseudomonads and the impact of traditional clean-in-place on biofilm removal

Srinithi Muthuraman *, Jon Palmer, Steve Flint

Food microbiology- biofilm research team, School of Food Technology and Natural Sciences, Massey University, 4412 Palmerston North, New Zealand

ARTICLE INFO

Keywords:
Pseudomonads
Biofilm
EPS
CIP process
Regrowth
Footprints

ABSTRACT

Pseudomonads are common psychrotrophic spoilage bacteria associated with dairy, poultry, and meat processing environments. They can multiply at low temperatures, 4–7 °C, producing thermostable spoilage enzymes. Pseudomonads form strong biofilms by producing higher EPS (Extracellular polymeric substances) at low temperatures. This study focused on the biofilm formation of pseudomonads at the air-liquid interface and their EPS removal. Two strong biofilm-forming isolates, (*Pseudomonas lundensis*) 3SM and (*Pseudomonas cedrina)* 20SM were allowed to form biofilms on stainless steel coupons in a CDC reactor under a continuous flow of nutrients at 4 °C over a week. The cell counts reached approximately 7.5 log CFU/cm^2. The biofilms formed at the air-liquid interface showed more visible biofilms, polysaccharides, and higher cell counts than those submerged in liquid. Cleaning the biofilms using 1 % NaOH at 70 °C resulted in viable bacterial cells below the detection limit. However, residual material termed biofilm "footprints" was present after cleaning and were analysed with SEM and FTIR. The SEM observations showed tightly packed robust biofilm cells before cleaning. Coupons treated with 55 °C water showed an upper layer of degraded cells. After treatment with 70 °C NaOH, organic material was still visible under SEM. Based on the FTIR observations, the EPS extracted from the control and treated coupons showed that the amount of biomolecules reduced after cleaning with NaOH, but the footprints still existed. The biofilm footprints led to the early appearance of biofilms at the air-liquid interface compared to new coupons exposed to strong biofilm-forming isolates. Cleaning with caustic can eliminate the cells, but the EPS from biofilms of pseudomonads is not completely removed, resulting in a possibility of regrowth when the new inoculum is introduced.

1. Introduction

Pseudomonads are common contaminants in dairy, which cause spoilage by producing thermostable enzymes and pigments (Raposo et al., 2016). Pseudomonads are known for their ability to form denser biofilms at psychrotrophic temperatures (Liu et al., 2023). Pseudomonads are strong EPS (Extracellular polymeric substances matrix) producers (Wickramasinghe et al., 2020). The EPS produced by pseudomonads are exploitable as a public good by other weak EPS producers and pathogens (Puga et al., 2018).

Pseudomonads produce large amounts of exopolysaccharides, and the biofilms of pseudomonads in the food industry are hard to remove. The EPS protects the biofilm cells from harsh sanitizing and cleaning agents (Santos Rosado Castro et al., 2021). Most of the biofilm elimination studies target the cells, while EPS is a real culprit that accounts for the regrowth and recurrence of the biofilms when new occupant cells are introduced (Deng et al., 2025).

The term "footprint" was used in the past to describe the polymeric material left on the surface after the bacterial cells are removed by shear forces or enzymes (Neu & Marshall, 1991). The bacterial cells are removed carefully from the surface, and the remaining adhesive polymers observed with TEM and SEM revealed that the footprint material on the surface matches the size of the cells nearby and some showed as clumps after cell removal due to the hydrophobic properties (Neu & Marshall, 1991).

The commonly used sanitation system in industry is cleaning-in-place (CIP). The CIP system is designed to remove the deposits on the interior surface of the equipment without dismantling (Tirpanci Sivri et al., 2023). The conventional CIP process includes water rinse, alkali cleaning with or without acid cleaning, and sanitation (Joseph et al., 2001). Alkaline cleaning solubilizes the fats, carbohydrates, and proteins. Caustic soda is the most effective alkaline cleaner removing

* Corresponding author.
E-mail address: s.muthuraman@massey.ac.nz (S. Muthuraman).

https://doi.org/10.1016/j.foodres.2025.118215
Received 10 April 2025; Received in revised form 23 December 2025; Accepted 23 December 2025
Available online 24 December 2025

microbial cells and organic foulants. 1 % NaOH is effective in restoring the initial membrane performance of membranes of the bioreactor (Tomczak et al., 2021). However, the biofilm EPS can protect the biofilm cells from CIP chemicals, including caustic soda due to reduced diffusivity (Tang et al., 2010). The CIP chemicals can effectively remove the proteins and fats from food residues. However, the EPS matrix in the biofilms differs from the food residues, and the EPS that remains after cleaning can serve as an attachment site for bacterial cells (Antoniou & Frank, 2005).

This study focused on a CIP with water rinse and alkali wash without acid cleaning. This study involved forming air-liquid interface biofilms of psychrotrophic pseudomonads under a continuous flow of nutrients at cold temperatures. This study explored the potential of biofilm EPS footprints to enhance the biofilm formation of the same isolates.

2. Materials and methods

2.1. Bacterial isolates and culture conditions

The two strong biofilm-forming isolates at cold temperatures, 3SM (*P. lundensis*) and 20SM (*P. cedrina*) were chosen for this study. These isolates were obtained from a dairy source, and the identifications were done with 16S rDNA sequencing using Bac27F(5′-AGAGTTTGATCCTGGCTCAG-3′) and 1492R(5′-TACGGYTACCTTGTTACGACTT-3′) primers.

2.2. CDC reactor conditions

The CDC reactor was used to grow a week-old biofilm. The CDC biofilm reactor (CBR 90; Biosurface Technologies, USA) was used with stainless-steel coupons (304 grade with 2B finish with a total surface area of 2.26 cm^2). The coupons were passivated (cleaned with 50 % nitric acid at 70 °C for 30 min), sonicated for 30 min, cleaned with ethanol and Trigene, and autoclaved at 121 °C. The reactor parts were assembled and autoclaved before use. The entire CDC reactor was kept at 4 °C. The growth media used were half-strength TSB (TSB, Difco™, Becton, Dickinson and Company, USA). The cultures were inoculated in TSB for 24 h to reach the OD_{600} of 0.05 ± 0.15 (approximately 3 log CFU/mL of cells). Two percent (2 %) of the overnight culture was added directly to the reactor beaker containing 400 mL of TSB (approximately 3 log CFU/mL). The flow rate of the reactor was set at 3.3 mL/min to achieve a mean residence time lower than the doubling time (supplementary file 1). The coupon holders were lifted and supported about an inch to create the air-liquid interface on the top coupons (A-L) and the remaining two coupons were submerged (L1 and L2) (Kumar et al., 2021).

2.3. Enumeration of biofilm cells

The reactor was allowed to run for seven days. The coupons containing holders were removed randomly every 24 h, and a blank holder was replaced to maintain the turbulence. The removed coupons were washed with 0.85 % physiological saline and transferred to the vials containing 900 µL of saline. After transferring the coupons, 1 g of sterile glass beads was added, and the vials were sonicated for 5 min. After sonication, the coupon-containing vials were vortexed vigorously to remove the cells from the coupons. One hundred microlitres (100 µL) of the contents from the vials were serially diluted and plated on the TSA (TSA, Difco™, Becton, Dickinson and Company, USA) plates at 30 °C for 24 h. The viable bacterial colonies were counted and expressed as log CFU/cm^2. The cell counts were compared between the A-L, L1 and L2 coupons each time.

2.4. Quantification of polysaccharides

After a week of incubation, the coupons containing biofilms were taken out. Two coupons from the A-L, L1, and L2 coupons were added to a vial containing 2 mL of sterile distilled water. The vials containing coupons were sonicated for 30 min. After sonication, the contents were transferred to Eppendorf tubes. The Eppendorf tubes were centrifuged at 12000*g* for 5 min (Hettich, Mikro 220R, Germany). The supernatant was collected and filtered using a 0.2 µm syringe filter (Minisart, Sartorius, Germany). Two millilitres (2 mL) of the filtered supernatant were pooled into 15 mL of centrifuge tubes (Falcon®, Corning Incorporated, USA). The extracted EPS fractions were stored at −80 °C for 8 h. These tubes were placed in a freeze-dryer (Labkits, Hongkong) overnight (Shelf temperature − 40 °C, vacuum pressure below 100 Pa). The freeze-dried EPS was stored in a desiccator.

2.4.1. Quantification of polysaccharides

Total polysaccharides in the freeze-dried EPS were measured using the Phenol sulfuric acid method (DuBois et al., 1956) and D-glucose as a standard.

Reagents.

5% Phenol	30 µL
98% Sulfuric acid	150 µL

The freeze-dried EPS samples were diluted with 100 µL of sterile distilled water. Fifty microliters of the diluted EPS samples were added to a well in 96-well plates. One hundred fifty microlitres (150 µL) of sulfuric acid were added, followed by 30 µL of phenol. The plates were shaken at room temperature for 5 min. Then, they were placed on hot plates at 90 °C for 5 min and cooled for 5 min. The absorbance was read at 490 nm. The total polysaccharides were expressed as µg/cm^2 and compared between the A-L, L1 and L2 coupons.

2.5. ClP system

The CIP process involved an initial hot water rinse, treating with NaOH, and a final water rinse (Table.1). Hot water at 55 °C and 1 % NaOH at 70 °C represent a typical CIP system. The water and NaOH were heated in a hotplate to reach the required temperatures. Sterile distilled water was used in this experiment to prepare NaOH. The inlet tube was inserted into the beakers containing CIP chemicals (hot water and NaOH), and the temperatures of the chemicals were confirmed (in the outlet tube) before connecting to the CDC reactor. The entire CDC reactor was cleaned using 1.2 L of water and circulated for at least 3 to 4 cycles at 300 rpm to reach a Reynolds number of more than 12,000. After the water rinse, 2 holders were taken out for the cell counts and two blank holders were inserted to maintain the flow. The same steps were followed for NaOH.

2.5.1. Reynolds number

The flow of the CDC reactor in this study was turbulent based on the Reynolds number (Table 1). The Reynolds number was calculated by.

$$Re = \upsilon D_h/\eta$$

Table 1
Reynolds numbers for biofilm growth and CIP.

RPM	Reynolds number	Function	Flow	Flow rate	Contact time
125	4239	Biofilm growth	Turbulent	3.3 mL /min	–
300	12,215	CIP	Turbulent	10 mL/ min	Water – 20 min NaOH -20 min Water- 5 min

(Where υ is the hydrodynamic velocity (m/s), ρ is the density of the fluid, which is 998.23 Kg/m^3, η is the kinematic viscosity 1.0023E-06 m^2/s. D_h is calculated using the outer radius (R_o) of 0.03 m and the inner radius of 0.0225 m (R_i) (Prabhukhot et al., 2024).

2.6. Microscopic observations

After a week of biofilm formation, the coupons were observed under an epifluorescence (Nikon- Eclipse Ni-L, Nikon instruments, USA) microscope (Filter- TRITC – excitation wavelength 540–555 nm, emission wavelength 570–620 nm) and SEM to view the biofilm architecture and the difference between the air-liquid interface coupons and submerged coupons. The SEM observations were done with JSM 6500F (Jeol, Australia) with 1000× and 5000× magnifications. The coupons were dried and carbon-coated before observing under SEM. After the CIP process, the coupons were observed again under both an epifluorescence microscope and SEM to view the cleaning efficiency of the CIP process.

Acridine orange (Acridine orange, BDH, England) was used for staining the coupons to view the cells and EPS under an epifluorescence microscope. The coupons were stained with acridine orange for 3 min. After that, the coupons were washed and air-dried. The stained coupons were observed under 1000× magnification. The images were processed using NIS-elements D software (Version 6.02.01(Build 1955), Nikon Instruments, USA) (Li et al., 2022; Muthuraman et al., 2025).

2.7. Attenuated Total reflection – Fourier-transform infrared spectroscopy (ATR-FTIR)

The isolated EPS from untreated coupons and CIP cleaned coupons from the air-liquid interface were used for ATR-FTIR analysis to observe the composition of footprints left after cleaning with water and NaOH. The acid-cleaned coupon was used as a control and observed directly under FTIR (Nicolet™, Thermofisher Scientific™, USA). FTIR parameters were as follows: acquisition range 2000–400 cm^{-1}, scanning times of 32 s, and resolution of 4 cm^{-1} (Li et al., 2022). The collected FTIR spectra was baseline corrected and normalized using OMNIC software (OMNIC, Thermofisher Scientific™, USA). Spectral deconvolution was performed using OriginPro software (Origin Pro 2025, 10.2 Origin Lab Corporation, USA) with Gaussian curve fitting for protein and polysaccharide peaks.

2.8. Reinoculation of the strong biofilm formers

After CIP, the reactor was treated with hot water at pasteurization temperature (72 °C) for 2 min until the water reached the reactor lid to enable the inactivation of any remaining cells. Four holders were removed from the CIP-cleaned reactor, and four holders containing clean coupons were inserted, and the holders were transferred to a new reactor beaker (Fig. 1). This was allowed to run at a 3.3 mL/min flow rate and 125 rpm with half-strength TSB for 24 h, and after 24 h 2 % inoculum was added to check the biofilm formation differences between untreated clean coupons (treated with 50 % nitric acid at 70 °C for 30 min, represents pristine surface) and CIP-treated coupons. The cell counts between the control coupons and CIP cleaned coupons were compared at each time point.

2.9. Data analysis

All the experiments were performed with at least three biological and three technical replicates, except for the cell count data. For the cell counts, coupons from two reactors were collected (three biological and two technical replicates) due to the sampling limitation after introducing an air-liquid interface. The normality of the cell counts data was confirmed using Shapiro-wilk test, and the Levene's test confirmed the homogeneity of variances. Therefore, one-way analysis of variance (ANOVA) was used to compare the means from all groups. The one-way ANOVA was used to evaluate significant differences among the variables using Tukey's test, which had a *p*-value below 0.05 and was considered statistically significant. Data analysis was implemented using SPSS statistical software (Version 29.0.2.0; IBM®, USA). FTIR data were processed using Origin Pro software.

3. Results

3.1. Visible biofilm formation

The visible biofilm formation on the CDC reactor coupons was observed from 24 h. At 24 h, no visible biofilms were seen in all three coupons. After 48 h, a thin visible line appeared on the air-liquid interface. At the end of 72 h, thick visible biofilms were observed on the A-L coupons and visible aggregates started to form on L1 coupons. At the end of 144 h, compared to submerged coupons, the A-L coupons showed denser visible biofilms (Fig. 2).

3.2. Biofilm cell enumeration

The isolates 3SM and 20SM were allowed to form biofilms on the CDC reactor coupons with half-strength TSB. The growth was monitored every 24 h until 168 h (Fig. 3). At 24 h, the cell counts from the A-L

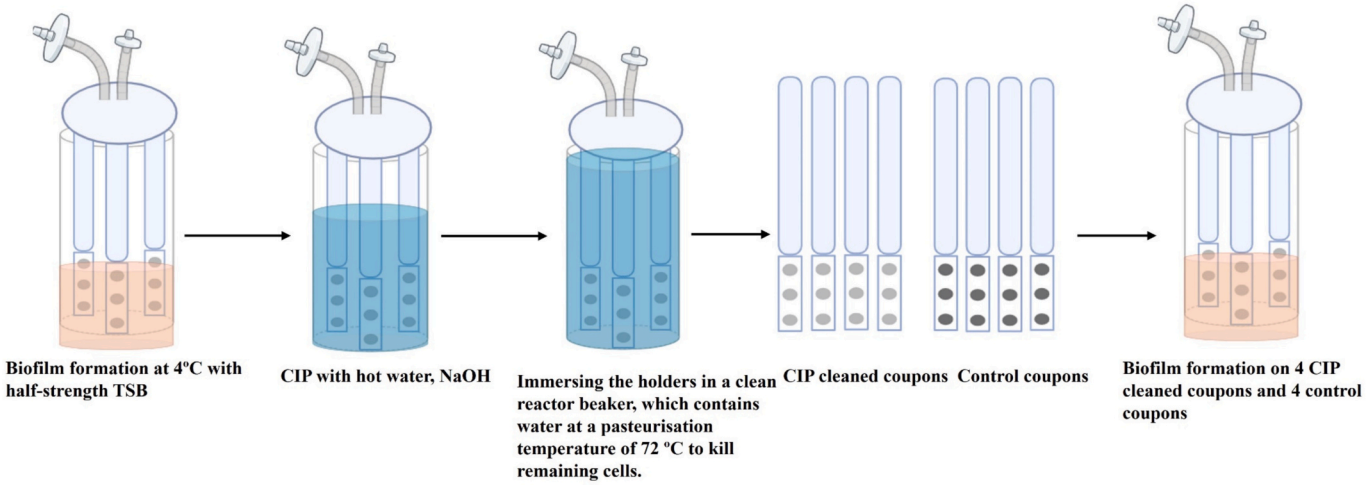

Fig. 1. Schematic representation of CIP and regrowth experimental setup.

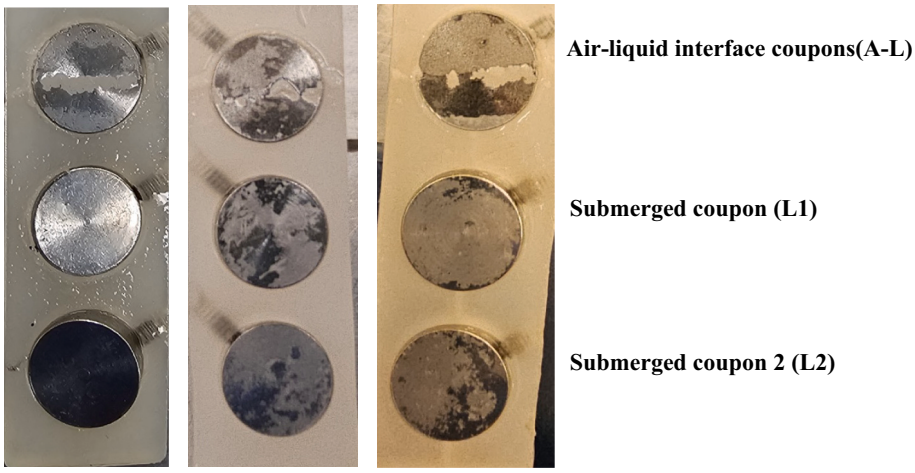

Fig. 2. The visible biofilm formation of isolate 3SM observed on A-L, L1, and L2 coupons at 168 h at 4 °C.

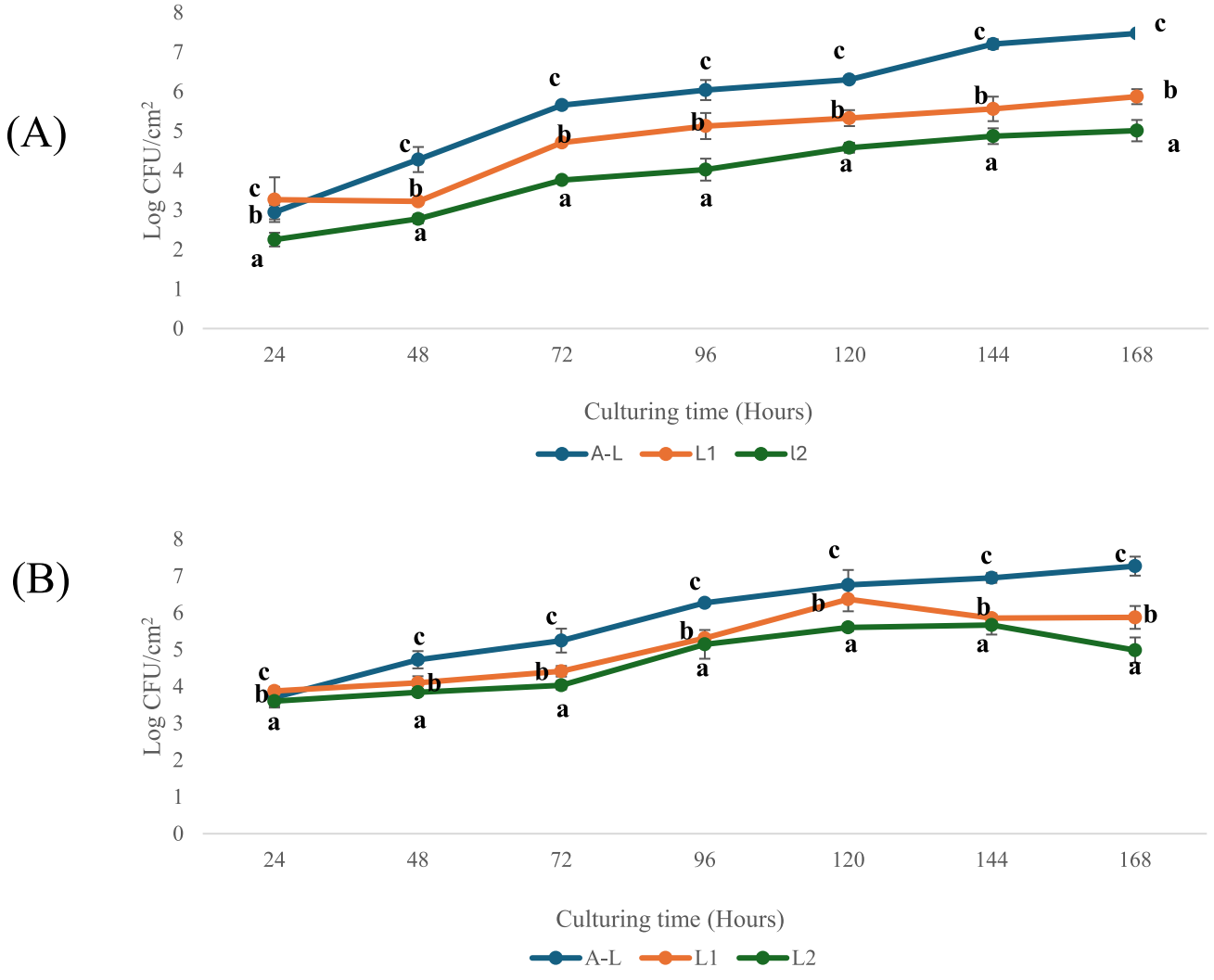

Fig. 3. Graph A shows the cell counts from isolate 3SM over seven days. Graph B shows the cell counts from the isolate 20SM. Different letters indicate significant differences ($p < 0.05$).

coupons were around 3.20 log CFU/cm^2 for both isolates. The L1 coupon also got similar cell counts at 24 h. From 48 h, the A-L coupons dominated in terms of cell counts compared to L1 and L2. This trend continued until the end of 168 h. At 168 h, the cell counts from the A-L coupons were around 7.26 and 7.47 log CFU/cm^2 for isolates 3SM and 20SM. At 168 h, the A-L coupons showed significantly higher cell counts ($p = 0.01$) compared to L1 and L2 coupons (Fig. 3).

3.3. Quantification of the polysaccharides

The EPS recovered from the A-L coupons was significantly ($p < 0.05$) higher than the L1 and L2 coupons (Fig. 4A). The total polysaccharides were also significantly higher ($p = 0.01$) in the biofilms formed at the A-L coupons compared to the L1 and L2 coupons (Fig. 4B). This indicates the importance of the air-liquid interface in EPS production by psychrotrophic pseudomonads.

3.4. Cell counts after CIP

The coupons were taken out after circulating hot water and again after NaOH. Hot water at 55 °C achieved around a log cell reduction in the biofilms formed by both the isolates. With NaOH, the cell counts were below the detectable limit (1.7 log CFU/cm^2) for both isolates. Compared to hot water at 55 °C, NaOH at 70 °C significantly ($p = 0.01$) killed the biofilm cells of psychrotrophic pseudomonads (Fig. 5).

3.5. Microscopic observations

3.5.1. Untreated coupons

With SEM observations, the biofilms produced by pseudomonads appeared as cells tightly packed together. With isolate 3SM, though the biofilms formed on A-L and L1 looked similar, the cell counts were significantly higher at the A-L coupons (Fig. 6A). However, with 20SM, the layers of cells were clearly seen on the A-L coupon (Fig. 6B), and on the L1 and L2 coupons, the stainless-steel surface was often seen between cell clusters. This observation agreed with the cell counts as the biofilms grown on A-L coupons showed more cells than the L1 and L2 coupons (Fig. 6A and B). However, this requires three-dimensional imaging to confirm the biofilm thickness differences between these two surfaces. With the epifluorescence microscopy, the cells on the A-L coupons were tightly packed and emitted higher fluorescence compared to the L1 and L2 coupons. Filamentous cells were present in all three coupons (Fig. 7A and B).

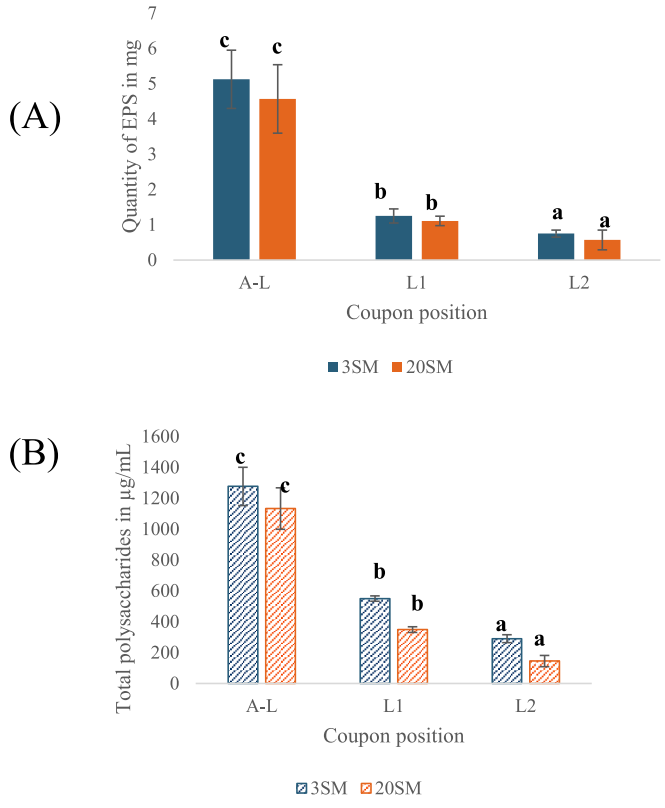

Fig. 4. Graph A shows the quantity of EPS recovered from the A-L, L1, and L2 coupons. Graph B shows the total polysaccharides from the isolated EPS recovered from A-L, L1, and L2 coupons. Different letters indicate significant differences ($p < 0.05$).

3.5.2. Cleaning with 55 °C water

With SEM observations, the hot water-treated coupon surfaces showed compromised upper layers on all the coupons. The cells can be seen but not as clear as the control coupons (untreated coupons with biofilm growth). The biomass appeared to be smeared (Fig. 6C and D). Cell counts after hot water treatment (55 °C for 10 min) resulted in one-log reduction. The cells after 55 °C treatment stayed intact, which was confirmed by epifluorescence microscopic observations, which agreed with the cell counts (Fig. 7C and D).

3.5.3. Cleaning with 70 °C NaOH

After introducing the NaOH to the CIP system, the coupons were free of live cells, which was confirmed by the SEM observation. However, the coupons were not completely clean. What appeared to be NaOH crystals, along with organic matter, were present in the coupons. These were the biofilm footprints left after cleaning (Fig. 6E and F). Compared to L1 and L2 coupons, the A-L coupons showed more organic materials left after cleaning. After cleaning with NaOH, the cell counts were below the detection limit (below 1.7 log CFU/cm^2). The acridine orange staining showed a dead and deformed mass on all three coupons (Fig. 7E and F).

3.6. ATR-FTIR spectra on EPS isolated from untreated and cleaned coupons

The FTIR spectra for the untreated and CIP-cleaned coupons were compared to the acid-cleaned stainless-steel coupon, which was used as a control. In the FTIR spectra, 1650 and 1540 cm-1 peaks represent the amide I and amide II bands of proteins and 1055 cm-1 from polysaccharides (Fig. 8A and B). Compared to the untreated EPS, the intensities of the respective peaks were decreased in EPS isolated from NaOH-treated coupons. With the hot water, the intensities did not decrease much for the polysaccharides but for proteins, however, there were some changes in the peaks noticed. The two peaks around 1400 and 1600 cm^{-1} in the untreated EPS become inverted in the hot water-treated EPS and the intensities of the protein peaks were decreased. The CIP-cleaned coupon was not as clean as the sterile acid-cleaned stainless-steel coupon. The presence of protein and polysaccharide peaks indicates the complex nature of the EPS even after CIP. The FTIR observation agreed with the remaining biofilm EPS footprints seen in SEM.

3.7. Regrowth of the strong biofilm former after CIP cleaning

Compared to the untreated clean coupons, the CIP cleaned coupons started showing a visible air-liquid interface from 24 h of incubation, whereas in clean coupons it took 72 h to form a visible air-liquid interface (Fig. 9C). The cell counts from the CIP-cleaned coupons were significantly ($p = 0.03$) higher than the control coupons from 24 h for both isolates. The cell counts in the A-L coupons of the CIP cleaned coupons were 6.71 ± 0.16 and 5.88 ± 0.13 log CFU/cm^2 for 3SM and 20SM, respectively (Fig. 9A and B). Whereas, in the control, clean coupons, the A-L coupons yielded 3.59 ± 0.17 and 3.40 ± 0.19 log CFU/cm^2 for isolates 3SM and 20SM, respectively. The L1 and L2 coupons of the CIP cleaned group showed significantly ($p = 0.019$) higher cell counts than the control group of submerged coupons. These results suggest that the remaining footprints of biofilm EPS encouraged the cells to establish the early air-liquid interface biofilm.

4. Discussion

Pseudomonads can form biofilms at various interfaces, including the air-liquid interface, solid-liquid interface, and liquid-liquid interfaces

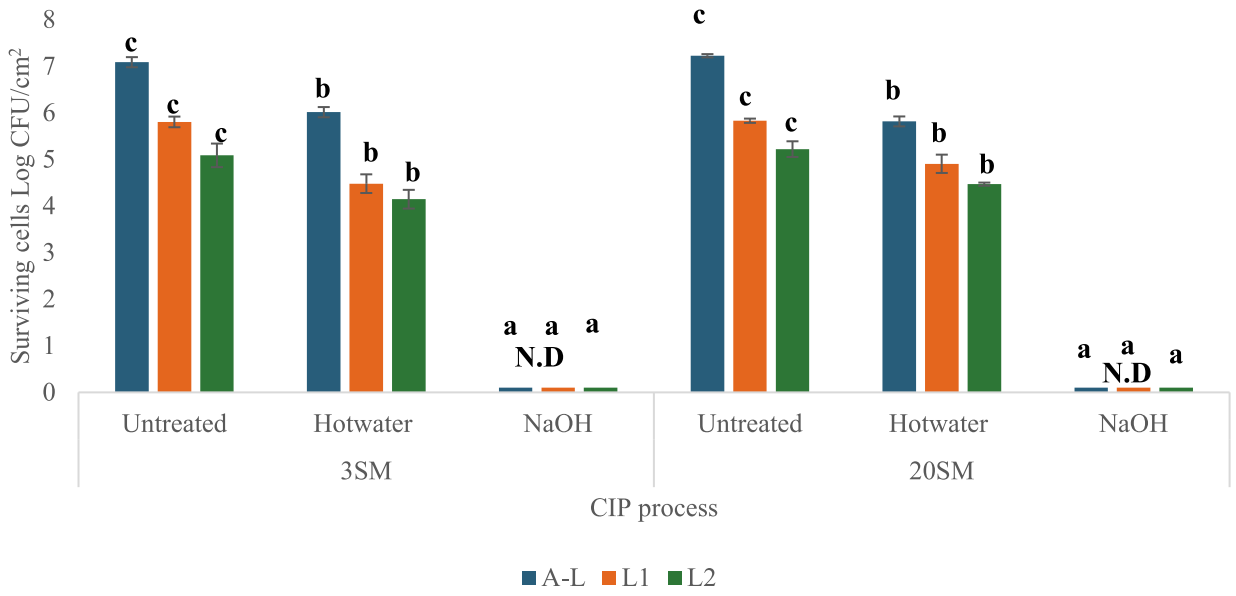

Fig. 5. The cell counts from untreated control coupons, hot water-treated coupons, and NaOH-treated coupons. Different letters indicate significant differences ($p < 0.05$).

(Robertson et al., 2013). The biofilm formation and cleaning studies on psychrotrophic pseudomonads in the food matrices mostly focused on the submerged biofilms (Liu et al., 2015; Liu et al., 2023). However, an air-liquid interface is commonly seen in food industries in partly filled silos, vats, balance tanks, stagnant water, etc. (Jha et al., 2020). This present study compared the biofilm formation between air-liquid interfaces and submerged biofilms. In this present study, introducing an air-liquid interface in the CDC reactor encouraged more cell counts and EPS production on the air-liquid interface coupons compared to the submerged coupons for both isolates. This present study showed that the CDC biofilm reactor can be used to grow air-liquid interface biofilms under a continuous flow of nutrients. However, when *P. aeruginosa* biofilms are grown in a CDC reactor, the coupon position does not affect the cell counts (Buckner et al., 2024). In another study comparing the biofilm formation of *Bacillus cereus* between air-liquid interface and submerged biofilms revealed that, compared to the submerged coupons, the air-liquid interface coupons showed significantly ($p < 0.05$) higher cell counts in both UHT milk and BHI media. The higher cell counts at the air-liquid interface are due to the aero taxis of bacteria to the surface, observed in *Bacillus* biofilms (Wijman et al., 2007).

In our previous study, these isolates produced higher polysaccharides in their EPS matrix compared to proteins and eDNA (Muthuraman et al., 2025). Other studies also reported that pseudomonads produce higher polysaccharides in their EPS matrix, and this present study focused on quantifying polysaccharides (Harimawan & Ting, 2016; Liu et al., 2023). In this present study, the quantity of isolated EPS and the total polysaccharides was higher in the A-L coupons compared to L1 and L2, which confirmed the link between the air-liquid interface and EPS production in pseudomonads. The thick visible biofilms at the air-liquid interface correlate with the EPS and polysaccharide quantification. This present study confirmed that the air-liquid interface encourages higher cell numbers and EPS production compared to the submerged biofilm formation. In a similar study with *B. cereus* mentioned that the EPS produced is higher in the semi-submerged coupons due to the gas-liquid interface (Ren et al., 2024). Comparison of the air-liquid interface biofilm formation of *P. fluorescens, B. cereus* and *B. subtilis* revealed that the *Bacillus* biofilms were of cell associations, while the *P. fluorescens* contained a higher amount of EPS (Constantin, 2010). In this present study, the pseudomonads produced higher cell counts and EPS production at the air-liquid interface, indicating higher EPS production observed with pseudomonad biofilms. This present study indicates the possibility of pseudomonads producing air-liquid interface biofilms with higher EPS in storage tanks, heat exchangers that are refrigerated and run under turbulent flow.

This study also focused on the CIP cleaning of mature biofilms. The cleaning and sanitation studies require mature, established biofilms and generating the robust biofilms is a critical step in designing the CIP process (Tirpanci Sivri et al., 2023). The time required to form these biofilms is also important in studying the CIP process. Most studies reported that the time to form mature biofilms in a static system or continuous flow reactor requires 18 h to 144 h (Bremer et al., 2006; Liu et al., 2023; Tirpanci Sivri et al., 2023). Among these studies, Liu et al. (2023) reported the biofilm formation of pseudomonads at cold temperature (at 4 °C, 144 h). However, the biofilms were formed on stainless-steel coupons in a static system. This present study found that even with a continuous flow of nutrients, the mature biofilms at cold temperatures require more than 144 h.

The biofilm removal of *P. aeruginosa* with ZnO nanoparticles revealed that the removal of the established biofilms requires higher concentrations of ZnO compared to the biofilm inhibition (Al-Momani et al., 2023). Considering these reasons, this present study focused on CIP cleaning of mature biofilms. This present study focused on biofilm removal with water and caustic. 1 % Caustic at 70 °C effectively removed all the cells, but the remaining biofilm footprints were noted on the surface from the microscopic observations. A similar study on the effects of cleaning regimes on biofilms of thermophilic bacilli on stainless steel showed that 2 % caustic for 30 min at 70 °C, followed by a water rinse and 1.8 % HNO_3 at 75 °C, removed the cells and polysaccharides effectively. This study also reported that the caustic treatment alone showed 6 log cell reductions. However, the fluorescent polysaccharide remnants were observed, indicating that caustic treatment failed to remove the biofilms completely (Parkar et al., 2004). A study on the removal *of P. putida* biofilms from stainless-steel surfaces using different concentrations of NaOH revealed that the cells are readily removed by the alkaline cleaners. However, mechanical scrubbing or high-pressure sprays are recommended for complete removal of EPS (Antoniou & Frank, 2005). The ineffectiveness of traditional CIP is reported by several other studies. A study with multi-species biofilms noted that there are survivors even after the final sanitation step, and the traditional CIP is ineffective in removing biofilms on the reverse osmosis membranes in dairy industries. The survivors were *Bacillus* isolates that can form spores and survive post-treatments (Singh & Anand, 2022). A

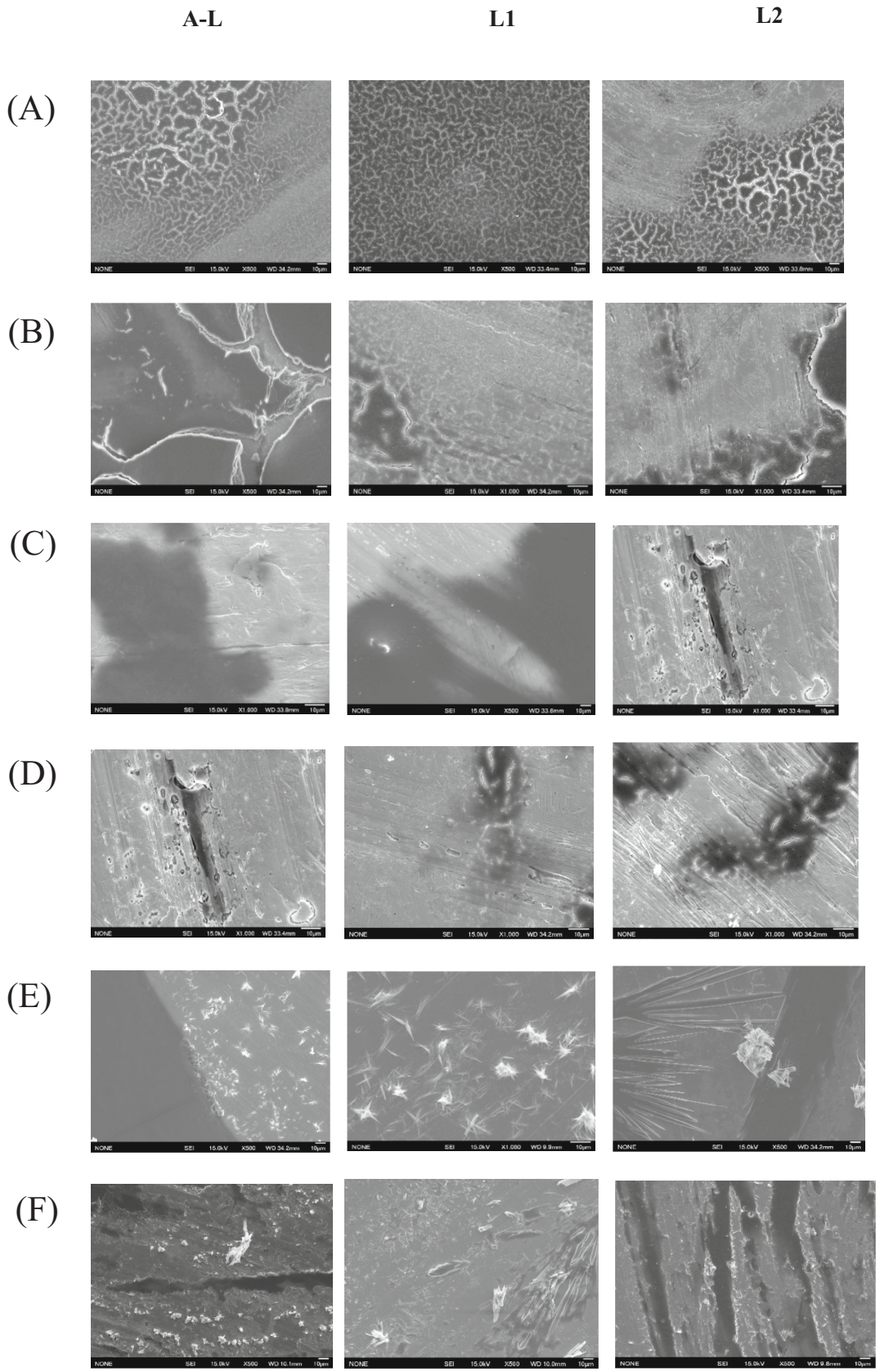

Fig. 6. (A)& (B) SEM images of 3SM and 20SM untreated coupons (Scale bar 10 μm), (C) & (D)SEM images of hot water-treated coupons of isolates 3SM and 20SM (Scale bar 10 μm), and (D) & (F) SEM images of NaOH-treated coupons of isolates 3SM and 20SM (Scale bar 1 μm).

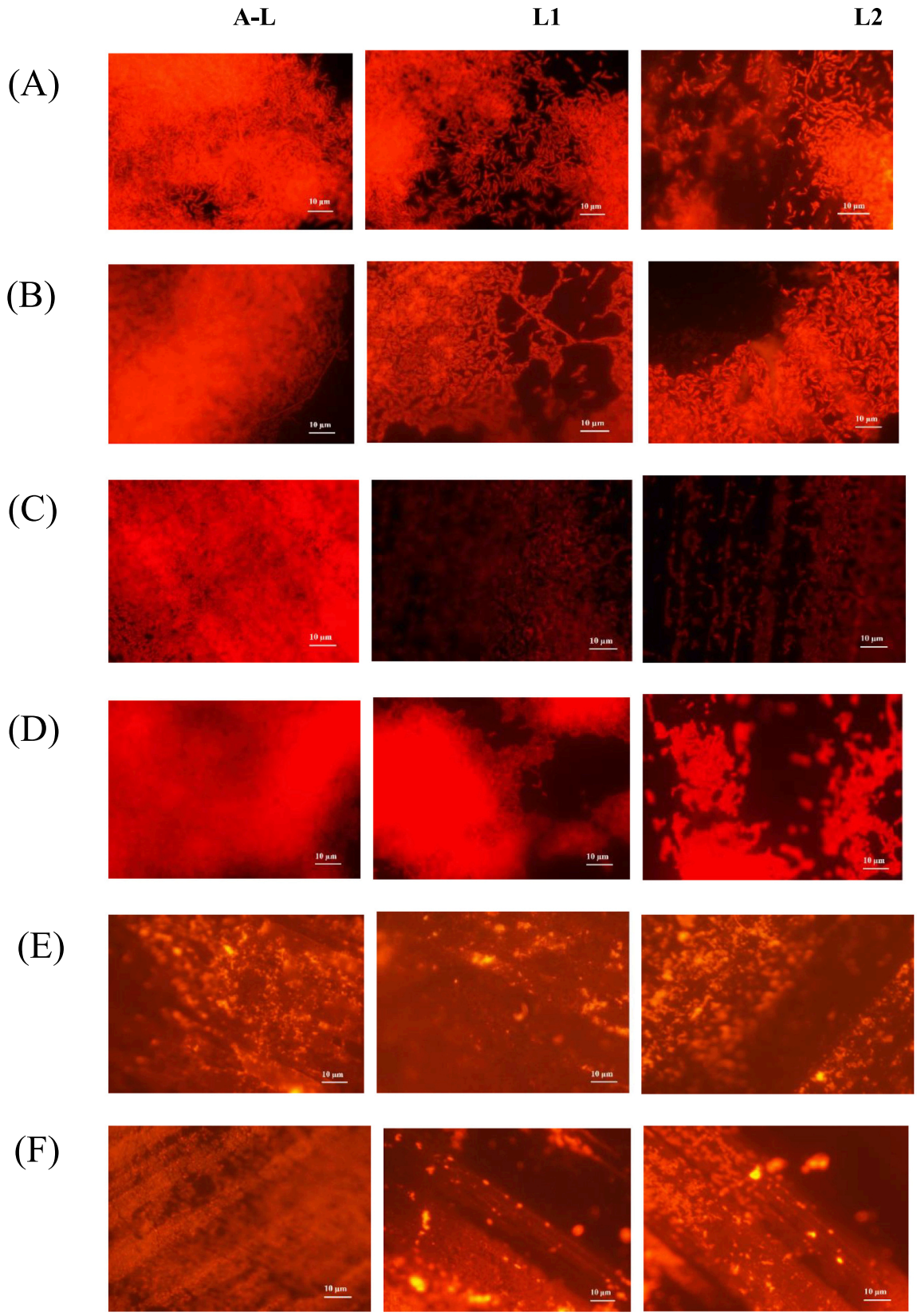

Fig. 7. (A) & (B) epifluorescence microscopic images of 3SM and 20SM untreated coupons, (C) & (D) hot water-treated coupons of isolates 3SM and 20SM, and (E) & (F) NaOH-treated coupons of isolates 3SM and 20SM (Scale bar 10 µm).

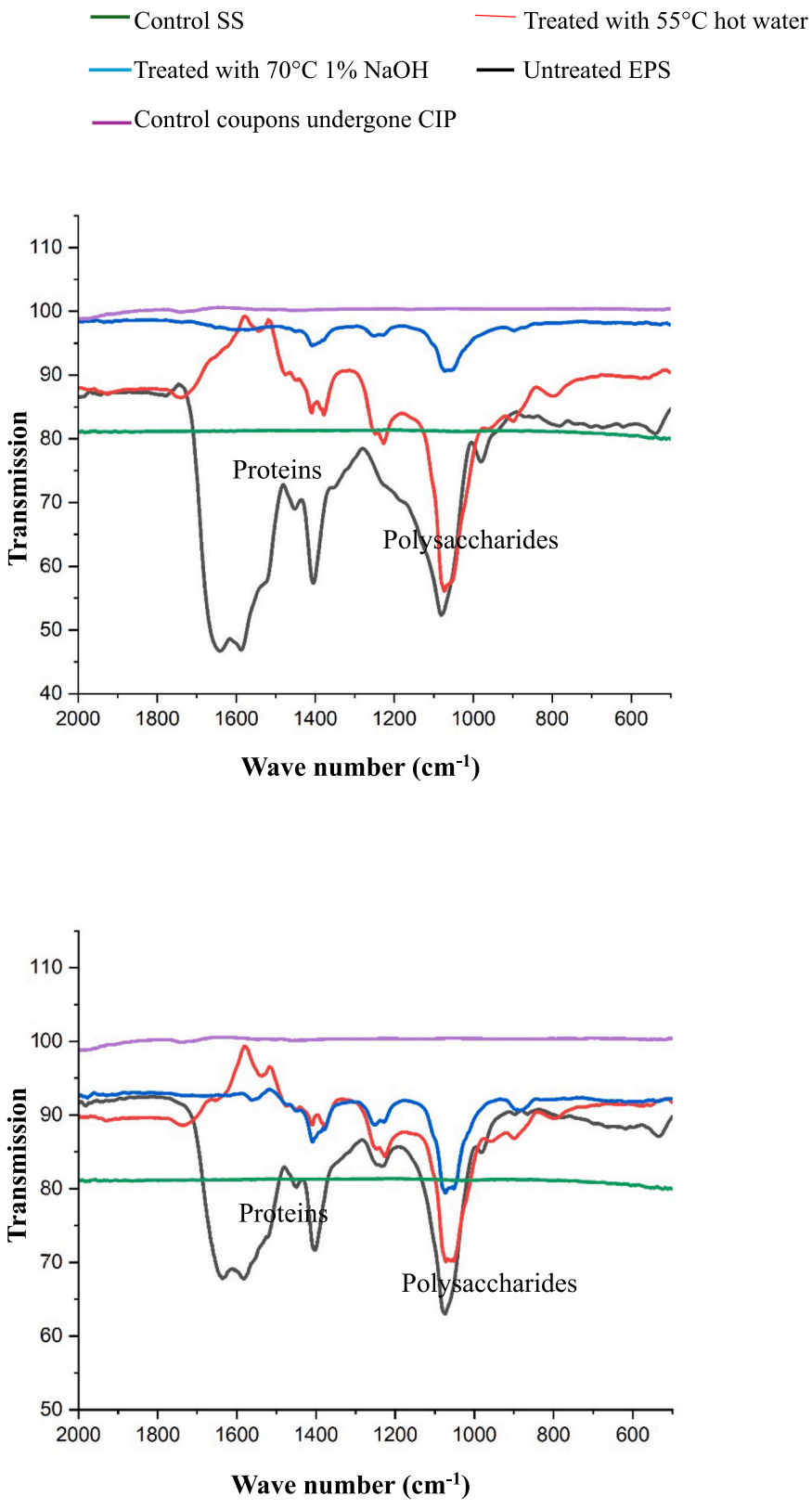

Fig. 8. (A) ATR-FTIR images of the untreated, hot water washed and NaOH washed coupons from isolate 3SM and (B)20SM.

study on *Klebsiella oxytoca* biofilms on ultrafiltration membranes showed that the traditional 6-step CIP process was not effective in removing the biofilms, and the culturable cells around 1.40–2.18 log CFU/cm^2 remained on the membrane surface (Tang et al., 2010). These observations suggest the need for additional mechanical or chemical treatments in the food industry for the complete removal of residual EPS. Our trials on treating the biofilms with NaOH and enzyme cleaners removed the EPS footprints, which reflected in the reinoculation

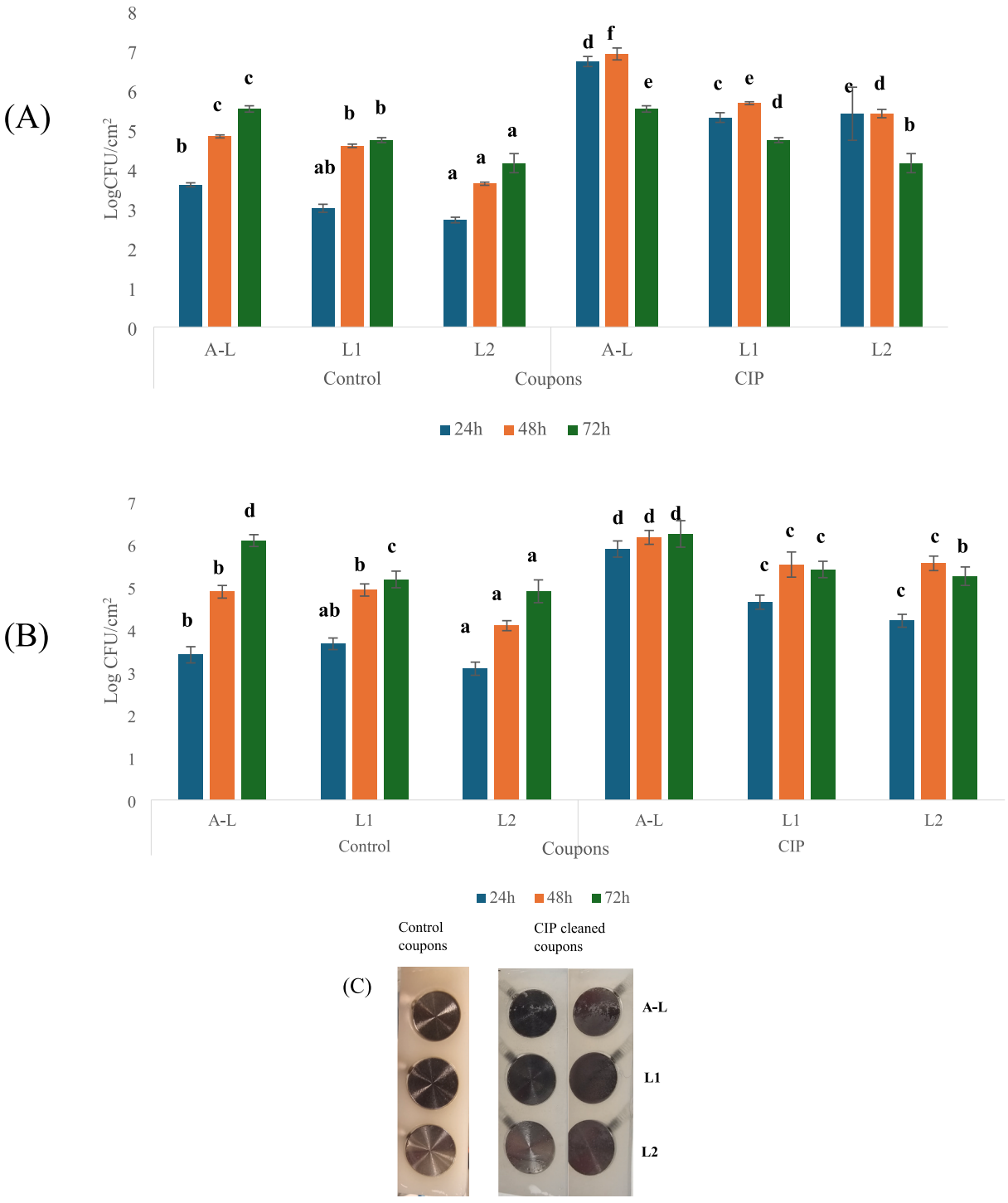

Fig. 9. Graph A shows the regrowth of isolate 3SM after CIP cleaning while Graph B shows the regrowth of isolate 20SM after CIP cleaning. All the results were expressed as mean ± standard deviation. Different letters indicate significant differences ($p < 0.05$), and (C) shows the early appearance of the air-liquid interface in the CIP-cleaned coupons of isolate 3SM.

(Supplementary File 1).

In this present study, the SEM results showed remaining EPS footprints and NaOH crystals for both the strong biofilm-forming isolates. The presence of NaOH crystals even after washing explains the possibility of NaOH deposits over time. A study on the removal of pseudomonad biofilms with microbubblers showed the remaining footprints of EPS with SEM observations (Deng et al., 2025). Treating the air-liquid interface biofilms of *P. fluorescens*, *B. cereus,* and *E.coli* with CIP chemicals and acridine orange staining showed that *P. fluorescens* contains higher biofilm debris and dead cells on the surface and no viability when tested, *E.coli* biofilm surface was clear, and *B. cereus* showed some spores and viable cells when plated (Jha et al., 2020). In this present study, with acridine orange, the pseudomonad biofilms showed similar results; dead cells and biofilm debris were present. This data suggests that pseudomonads are among the strong EPS producers, and their EPS is hard to remove from the surface.

With FTIR data, in this present study, the CIP-cleaned coupons of both isolates were not as clean as the acid-cleaned control coupons.

Peaks for polysaccharides and proteins can be seen after cleaning with caustic soda, which supports that the footprints can be present even after treating with caustic. Peaks for both polysaccharides and proteins revealed that the complex nature of the EPS remains the same even after CIP. Similar observations were seen in a study treating *P. aeruginosa* biofilms with DDAB (Didecyl Dimenthyl Ammonium Bromide) and SAEW (Slightly Acidic Electrolysed Water). Even if cell removal is achieved, removing EPS footprints from the surface is harder (Li et al., 2022).

This present study also demonstrated the early appearance of an air-liquid interface biofilm with strong biofilm-forming isolates. The submerged CIP coupons L1 and L2 showed significantly higher cell counts than the control coupons. Regardless of the coupon positions, all three coupons encouraged more aggressive regrowth after introducing new inoculum. However, the cell counts from the A-L CIP coupons were significantly higher than those from the L1 and L2 CIP coupons. Similarly, in a study with cassia essential oil combined with amylase and proteinase, significantly removed the viable cells of *Salmonella* and *Listeria* spp. However, the regeneration of the biofilms was observed within 24 h with high cell density, higher EPS production, and robust biofilm formation (Cervantes-Huamán et al., 2025). When the multispecies biofilm grown on titanium surfaces is cleaned with antimicrobials, the regrowth of the biofilms after introducing the new inoculum appears early and aggressive (Han et al., 2019). These observations indicate the potential of EPS in the aggressive biofilm formation of upcoming cells or colonizers. This present study confirmed that not only the air-liquid interface, but even the submerged biofilms were hard to eliminate and can support the reinoculation effectively.

However, the cleaning and sanitation studies mostly focused on the bactericidal effects and the role of EPS is often ignored (Bénézech & Faille, 2018; Medina-Rodríguez et al., 2020). Even after treating the biofilms of *E. coli* and *S. aureus* with cold plasma, the microscopic observations revealed that the polysaccharides, proteins and eDNA contents were reduced but not completely removed (Xia et al., 2024). This present study focused on the EPS rather than cells by exploring the role of EPS in aggressive regrowth. A similar study on biofilm eradication of *P. aeruginosa* EPS removal and regrowth showed that microbubblers have the potential to invade, deform, and displace EPS by 99.9 %. Self-locomotive MnO_2 doped diatom micro-bubblers activated by H_2O_2 are known as SLAM. SLAM, when combined with peracetic acid (PAA) and H_2O_2, shows promising results against *P. aeruginosa* biofilms and prevents the regrowth over time by reducing the EPS volume (Deng et al., 2025). However, the SLAM is in the initial stage of research, and there is a need to develop easy and adaptable strategies to remove these EPS footprints.

This present study focused on psychrotrophic pseudomonads that are non-spore formers and can be killed with heat treatment. However, in industries, bacteria exist as multispecies community biofilms, and there might be cells that cannot be killed by heat treatment, and some of them can produce spores. There is a need for more studies to analyze the footprints in a multispecies setup, including thermophilic bacteria. Even though this present study focused on the mature biofilms of strong biofilm formers, strain diversity needs to be considered. The changes in gene expression during footprint-mediated biofilm formation need to be studied to understand the role of EPS footprints. This present study explored the consequences of remaining biofilm EPS footprints; however, studies targeting the removal of biofilm footprints need to be developed.

5. Conclusion

This study showed the reason behind the ineffectiveness of caustic soda against biofilm removal. The pseudomonads used in this study can be killed by hot water and caustic treatment. However, the remaining biofilm footprints can encourage the biofilm formation of the same isolate. The regenerated biofilm was more aggressive than the previous biofilm. Targeting the removal of remaining biofilm footprints after the CIP process or any other antimicrobial treatments needs to be developed.

CRediT authorship contribution statement

Srinithi Muthuraman: Writing – review & editing, Writing – original draft, Methodology, Investigation, Formal analysis, Conceptualization. **Jon Palmer:** Writing – review & editing, Supervision, Conceptualization. **Steve Flint:** Writing – review & editing, Supervision, Conceptualization.

Declaration of competing interest

The authors declare that they have no known competing financial interests or personal relationships that could have appeared to influence the work reported in this paper.

Appendix A. Supplementary data

Supplementary data to this article can be found online at https://doi.org/10.1016/j.foodres.2025.118215.

Data availability

Data will be made available on request.

References

Al-Momani, H., Al Balawi, D., Hamed, S., Albiss, B. A., Almasri, M., AlGhawrie, H., … Ward, C. (2023). The impact of biosynthesized ZnO nanoparticles from Olea europaea (common olive) on *Pseudomonas aeruginosa* growth and biofilm formation. *Scientific Reports, 13*(1), 5096. https://doi.org/10.1038/s41598-023-32366-1

Antoniou, K., & Frank, J. F. (2005). Removal of *Pseudomonas putida* biofilm and associated extracellular polymeric substances from stainless steel by alkali cleaning. *Journal of Food Protection, 68*(2), 277–281. https://doi.org/10.4315/0362-028x-68.2.277

Bénézech, T., & Faille, C. (2018). Two-phase kinetics of biofilm removal during CIP. Respective roles of mechanical and chemical effects on the detachment of single cells vs cell clusters from a *Pseudomonas fluorescens* biofilm. *Journal of Food Engineering, 219*, 121–128.

Bremer, P. J., Fillery, S., & McQuillan, A. J. (2006). Laboratory scale clean-in-place (CIP) studies on the effectiveness of different caustic and acid wash steps on the removal of dairy biofilms. *International Journal of Food Microbiology, 106*(3), 254–262. https://doi.org/10.1016/j.ijfoodmicro.2005.07.004

Buckner, E., Buckingham-Meyer, K., Miller, L. A., Parker, A. E., Jones, C. J., & Goeres, D. M. (2024). Coupon position does not affect *Pseudomonas aeruginosa* and *Staphylococcus aureus* biofilm densities in the CDC biofilm reactor. *Journal of Microbiological Methods, 223*, Article 106960. https://doi.org/10.1016/j.mimet.2024.106960

Cervantes-Huamán, B. R. H., Vega-Sánchez, A., Rolón-Verdún, P., Gervilla-Cantero, G., Rodríguez-Jerez, J. J., & Ripolles-Avila, C. (2025). Effect of Cinnamomum cassia essential oil combined with enzymes on the elimination and regrowth potential of *Listeria monocytogenes* and *Salmonella enterica* biofilms formed on stainless steel surfaces. *Food Control, 172*, Article 111120. https://doi.org/10.1016/j.foodcont.2024.111120

Constantin, O. E. (2010). Air-Liquid Interface Biofilms of Bacillus cereus, Bacillus subtilis and Pseudomonas fluorescens. *Journal of Agroalimentary Processes and Technologies, 16*(3), 317–320.

Deng, Y.-H., Lee, J. H., Kim, M.-J., & Kong, H. (2025). Biofilm comes back: Controlling regrowth by mitigating the cell-matrix interaction. *Chemical Engineering Journal, 508*, Article 160947. https://doi.org/10.1016/j.cej.2025.160947

Dubois, M., Gilles, K. A., Hamilton, J. K., Rebers, P. A., & Smith, F. (1956). Colorimetric method for determination of sugars and related substances. *Analytical Chemistry, 28*(3), 350–356. https://doi.org/10.1021/ac60111a017

Han, Q., Jiang, Y., Brandt, B. W., Yang, J., Chen, Y., Buijs, M. J., … Deng, D. (2019). Regrowth of microcosm biofilms on titanium surfaces after various antimicrobial treatments. *Frontiers in Microbiology, 10*, 2693. https://doi.org/10.3389/fmicb.2019.02693

Harimawan, A., & Ting, Y.-P. (2016). Investigation of extracellular polymeric substances (EPS) properties of *P. Aeruginosa* and *B. Subtilis* and their role in bacterial adhesion. *Colloids and Surfaces B: Biointerfaces, 146*, 459–467. https://doi.org/10.1016/j.colsurfb.2016.06.039

Jha, P. K., Dallagi, H., Richard, E., Benezech, T., & Faille, C. (2020). Formation and resistance to cleaning of biofilms at air-liquid-wall interface. Influence of bacterial strain and material. *Food Control, 118*, Article 107384. https://doi.org/10.1016/j.foodcont.2020.107384

Joseph, B., Otta, S. K., Karunasagar, I., & Karunasagar, I. (2001). Biofilm formation by *Salmonella* spp. on food contact surfaces and their sensitivity to sanitizers. *International Journal of Food Microbiology, 64*(3), 367–372. https://doi.org/10.1016/S0168-1605(00)00466-9

Li, Y., Wang, H., Zheng, X., Li, Z., Wang, M., Luo, K., Zhang, C., Xia, X., Wang, Y., & Shi, C. (2022). Didecyldimethylammonium bromide: Application to control biofilms of *Staphylococcus aureus* and *Pseudomonas aeruginosa* alone and in combination with slightly acidic electrolyzed water. *Food Research International, 157*, Article 111236. https://doi.org/10.1016/j.foodres.2022.111236

Liu, J., Wu, S., Feng, L., Wu, Y., & Zhu, J. (2023). Extracellular matrix affects mature biofilm and stress resistance of psychrotrophic spoilage *Pseudomonas* at cold temperature. *Food Microbiology, 112*, Article 104214. https://doi.org/10.1016/j.fm.2023.104214

Liu, Y., Xie, J., Zhao, L., Qian, Y., Zhao, Y., & Liu, X. (2015). Biofilm formation characteristics of *Pseudomonas lundensis* isolated from meat. *Journal of Food Science, 80*(12). https://doi.org/10.1111/1750-3841.13142

Medina-Rodríguez, A. C., Ávila-Sierra, A., Ariza, J. J., Guillamón, E., Baños-Arjona, A., Vicaria, J. M., & Jurado, E. (2020). Clean-in-place disinfection of dual-species biofilm (*Listeria* and *Pseudomonas)* by a green antibacterial product made from citrus extract. *Food Control, 118*, Article 107422.

Muthuraman, S., Flint, S., & Palmer, J. (2025). Characterization of the extracellular polymeric substances matrix of *Pseudomonas* biofilms formed at the air-liquid interface. *Food Bioscience, 64*, Article 105918. https://doi.org/10.1016/j.fbio.2025.105918

Neu, T. R., & Marshall, K. C. (1991). Microbial "footprints"—A new approach to adhesive polymers. *Biofouling, 3*(2), 101–112. https://doi.org/10.1080/08927019109378166

Parkar, S. G., Flint, S. H., & Brooks, J. D. (2004). Evaluation of the effect of cleaning regimes on biofilms of thermophilic bacilli on stainless steel. *Journal of Applied Microbiology, 96*(1), 110–116. https://doi.org/10.1046/j.1365-2672.2003.02136.x

Prabhukhot, G. S., Eggleton, C. D., Kim, M., & Patel, J. (2024). Impact of surface topography and hydrodynamic flow conditions on single and multispecies biofilm formation by *Escherichia coli* O157:H7 and *Listeria monocytogenes* in presence of promotor bacteria. *LWT, 201*, Article 116240. https://doi.org/10.1016/j.lwt.2024.116240

Puga, C. H., Dahdouh, E., SanJose, C., & Orgaz, B. (2018). *Listeria monocytogenes* colonizes *Pseudomonas fluorescens* biofilms and induces matrix over-production. *Frontiers in Microbiology, 9*, 1706. https://doi.org/10.3389/fmicb.2018.01706

Raposo, A., Pérez, E., De Faria, C. T., Ferrús, M. A., & Carrascosa, C. (2016). Food spoilage by *Pseudomonas* spp.—An overview. In O. V. Singh (Ed.), *Foodborne pathogens and antibiotic resistance* (1st ed., pp. 41–71). Wiley. https://doi.org/10.1002/9781119139188.ch3.

Ren, F., Chen, Y., Yang, S., Zhang, Y., Liu, Y., Ma, Y., Wang, Y., Liu, Y., Dong, Q., & Lu, D. (2024). Characterization of emetic *Bacillus cereus* biofilm formation and cereulide production in biofilm. *Food Research International, 192*, Article 114834. https://doi.org/10.1016/j.foodres.2024.114834

Robertson, M., Hapca, S. M., Moshynets, O., & Spiers, A. J. (2013). Air–liquid interface biofilm formation by psychrotrophic pseudomonads recovered from spoilt meat. *Antonie Van Leeuwenhoek, 103*(1), 251–259. https://doi.org/10.1007/s10482-012-9796-x

Santos Rosado Castro, M., Da Silva Fernandes, M., Kabuki, D. Y., & Kuaye, A. Y. (2021). Modelling *Pseudomonas fluorescens* and *Pseudomonas aeruginosa* biofilm formation on stainless steel surfaces and controlling through sanitisers. *International Dairy Journal, 114*, Article 104945. https://doi.org/10.1016/j.idairyj.2020.104945

Singh, D., & Anand, S. (2022). Efficacy of a typical clean-in-place protocol against in vitro membrane biofilms. *Journal of Dairy Science, 105*(12), 9417–9425. https://doi.org/10.3168/jds.2022-21712

Tang, X., Flint, S. H., Bennett, R. J., & Brooks, J. D. (2010). The efficacy of different cleaners and sanitisers in cleaning biofilms on UF membranes used in the dairy industry. *Journal of Membrane Science, 352*(1–2), 71–75. https://doi.org/10.1016/j.memsci.2010.01.063

Tirpanci Sivri, G., Abdelhamid, A. G., Kasler, D. R., & Yousef, A. E. (2023). Removal of *Pseudomonas fluorescens* biofilms from pilot-scale food processing equipment using ozone-assisted cleaning-in-place. *Frontiers in Microbiology, 14*, Article 1141907. https://doi.org/10.3389/fmicb.2023.1141907

Tomczak, W., Grubecki, I., & Gryta, M. (2021). The use of NaOH solutions for fouling control in a membrane bioreactor: A feasibility study. *Membranes, 11*(11), 887. https://doi.org/10.3390/membranes11110887

Wickramasinghe, N. N., Hlaing, M. M., Ravensdale, J. T., Coorey, R., Chandry, P. S., & Dykes, G. A. (2020). Characterization of the biofilm matrix composition of psychrotrophic, meat spoilage pseudomonads. *Scientific Reports, 10*(1), 16457. https://doi.org/10.1038/s41598-020-73612-0

Wijman, J. G. E., De Leeuw, P. P. L. A., Moezelaar, R., Zwietering, M. H., & Abee, T. (2007). Air-liquid Interface biofilms of *Bacillus cereus*: Formation, sporulation, and dispersion. *Applied and Environmental Microbiology, 73*(5), 1481–1488. https://doi.org/10.1128/AEM.01781-06